AIP | Journal of Applied Physics

Optical and reduced band gap in n- and p-type GaN and AlN

C. Persson, Bo E. Sernelius, A. Ferreira da Silva, C. Moysés Araújo, R. Ahuja et al.

Citation: J. Appl. Phys. 92, 3207 (2002); doi: 10.1063/1.1504499
View online: http://dx.doi.org/10.1063/1.1504499
View Table of Contents: http://jap.aip.org/resource/1/JAPIAU/v92/i6
Published by the American Institute of Physics.

Related Articles

Competitive carrier interactions influencing the emission dynamics of GaAsSb-capped InAs quantum dots
Appl. Phys. Lett. 101, 231109 (2012)

Observation of momentum space semi-localization in Si-doped β-Ga2O3
Appl. Phys. Lett. 101, 232105 (2012)

Role of the dimensionality of the [GaX]2 network in the Zintl phases EuGa2X2
J. Appl. Phys. 112, 103714 (2012)

An investigation of the Young's modulus of single-crystalline wurtzite indium nitride using an atomic force microscopy based micromechanical bending test
Appl. Phys. Lett. 101, 221906 (2012)

Temperature and Bi-concentration dependence of the bandgap and spin-orbit splitting in InGaBiAs/InP semiconductors for mid-infrared applications
Appl. Phys. Lett. 101, 221108 (2012)

Additional information on J. Appl. Phys.

Journal Homepage: http://jap.aip.org/
Journal Information: http://jap.aip.org/about/about_the_journal
Top downloads: http://jap.aip.org/features/most_downloaded
Information for Authors: http://jap.aip.org/authors

ADVERTISEMENT

Downloaded 12 Dec 2012 to 200.128.60.106. Redistribution subject to AIP license or copyright; see http://jap.aip.org/about/rights_and_permissions

Optical and reduced band gap in *n*- and *p*-type GaN and AlN

C. Persson[a)]
Condensed Matter Theory Group, Department of Physics, Uppsala University, Box 530, SE-751 21 Uppsala, Sweden and Department of Materials Science and Engineering, Royal Institute of Technology, SE-100 44 Stockholm, Sweden

Bo E. Sernelius
Solid State Division, Oak Ridge National Laboratory, Oak Ridge, Tennessee 37831-6032

A. Ferreira da Silva and C. Moysés Araújo
Instituto de Fisica, Universidade Federal da Bahia, Campus, Universitario de Ondina, 40210-340 Salvador, Bahia, Brazil

R. Ahuja
Condensed Matter Theory Group Department of Physics, Uppsala University, Box 530, Uppsala, Sweden

B. Johansson
Condensed Matter Theory Group, Department of Physics, Uppsala University, Box 530, SE-751 21 Uppsala, Sweden and Department of Materials Science and Engineering, Royal Institute of Technology, SE-100 44 Stockholm, Sweden

(Received 5 July 2002; accepted for publication 10 July 2002)

We present a full band calculation of the doping-induced energy shifts of the conduction-band minimum and the valence-band maximum for *n*- and *p*-type GaN and AlN. Both wurtzite and zinc-blende structures have been considered. The resulting optical and reduced band-gap energies are presented as functions of the ionized impurity concentration in the heavily doped regime. The computational method is based on a zero-temperature Green's function formalism within the random phase approximation and with the local-field correction of Hubbard. The calculation goes beyond the spherical approximation of the energy bands by using energy dispersions and overlap integrals from a first-principle, full-potential band-structure calculation. Inclusion of the spin-orbit interaction is crucial for describing the uppermost valence bands properly, and we show that the nonparabolicity of the valence bands influences the energy shifts strongly, especially the shift of the optical band gap. With the full band structure, we can explain the results of photoluminescence measurements by Yoshikawa *et al.* [J. Appl. Phys. **86**, 4400 (1999)]. © *2002 American Institute of Physics.* [DOI: 10.1063/1.1504499]

I. INTRODUCTION

The III nitrides are wide-band-gap semiconductor materials with low compressibility, good thermal stability, and with chemical and radiation inertness.[1,2] The comprehensive investigations of the wurtzite (wz) structures have led to commercial optoelectronic devices like GaN-based light-emitting diodes and detectors working in the visible–ultraviolet region,[1–3] as well as metal–semiconductor field-effect transistors.[4] As a result of the recent progress in crystal growth, one can also produce thin films of zinc-blende (zb) crystals,[5–7] which opens up for further technological applications involving III-nitride alloys. In order to design semiconductor devices properly, the effects on the semiconductor properties due to doping have to be made clear since doping can modify the band structure strongly.[8,9]

First, consider an undoped semiconductor where the Hamiltonian $\hat{H}_0$ describes the interactions between the ions and the electrons of the intrinsic crystal. The eigenvalue problem of $\hat{H}_0$ results in the single-electron energies $E_j^0(\mathbf{k})$ for the electron states with wave vector $\mathbf{k}$ in the jth band. The fundamental band gap E_g^0 is the lowest energy needed to promote one electron from the valence band to the conduction band (not considering the excitons). In an *n*-type semiconductor, the crystal also consists of shallow donors which can be ionized thermally. However, also in the zero-temperature limit the donors are fully ionized if the dopant concentration is above the critical concentration N_c for the metal–nonmetal (MNM) Mott transition.[10] The electrons associated with the ionized donors give rise to a "gas" of free electrons in the conduction band. The crystal electrons interact with the electron gas and the ionized donors strongly. Since the III nitrides are polar materials, these interactions are screened by the optical phonons. The additional interactions can be treated as a perturbation to $\hat{H}_0$, that is, $\hat{H}=\hat{H}_0+\hat{H}_1$ where $\hat{H}_1$ is the perturbation Hamiltonian describing the additional interactions. The eigenvalue problem of $\hat{H}$ yields the single-electron energies $E_j(\mathbf{k})$. The energy shift $E_j(\mathbf{k})-E_j^0(\mathbf{k})=\Delta E_j(\mathbf{k})=\mathrm{Re}[\hbar\Sigma_j(\mathbf{k},E_j^0(\mathbf{k})/\hbar)]$ is the real part of the self-energy of the electron state. Electron states in both the conduction and the valence bands (one needs at least one hole in the valence band to measure the band gap) are affected by the additional screening of the electron gas.

[a)]Electronic mail: clas.persson@fysik.uu.se

 © 2002 American Institute of Physics

Downloaded 12 Dec 2012 to 200.128.60.106. Redistribution subject to AIP license or copyright; see http://jap.aip.org/about/rights_and_permissions

Normally, the self-energy of a conduction-band state is negative and the self-energy of a valence-band state is positive, thereby yielding a smaller band gap: $E_g < E_g^0$. The description for *n*-type materials has a direct analogue for *p*-type materials.

In the present work, the energy shifts of the conduction-band minimum and of the valence-band maximum have been calculated as functions of ionized impurity concentration for *n*- and *p*-type wz-GaN, wz-AlN, zb-GaN, and zb-AlN. The self-energies have been worked out within the random phase approximation (RPA) with a local-field correction of Hubbard.[11–13] A simple approach to incorporate the electronic structure of the intrinsic crystal [i.e., $E_j^0(\mathbf{k})$] would be to use spherical energy dispersions. Also the overlap integrals, contained in the description of the electron–electron and electron-impurity ion interactions, can be parametrized within the spherical approximation. However, in this work, we have used the full energy dispersions and the overlap integrals obtained from a relativistic, full-potential band-structure calculation. We show that the nonparabolicity of the valence bands affects the calculated self-energies of the valence-band maximum. Moreover, in order to calculate accurately the optical band gap for semiconductors with direct band gap, it is crucial to include a full description of the uppermost valence bands. With the complete band structure we can give a reliable explanation of the photoluminescence (PL) results of wz-GaN:Si, presented by Yoshikawa *et al.*,[14] as zero-phonon-induced recombinations of electrons in the conduction band and nonthermalized holes in the three uppermost valence bands.

Throughout the article CGS units have been employed. We have taken into account the lowest conduction band ($c1$) and the three uppermost valence bands ($v1$, $v2$, and $v3$, where $v1$ is the uppermost band). In cubic materials, $v1$, $v2$, and $v3$ correspond to heavy-hole, light-hole, and spin-orbit split-off bands, respectively.

II. COMPUTATIONAL METHOD

The employed method for calculating the self-energy is by means of the RPA[11,12] with a local-field correction of Hubbard.[13] We have considered interactions caused by the electron–electron exchange–correlation interaction, the electron-ionized impurity attraction, and the optical-phonon screening. A zero-temperature formalism has been used and the temperature enters our model only through its capability to ionize the shallow impurities below the critical concentration for the Mott transition. Above the critical concentration the impurities are fully ionized even at zero absolute temperature. The concentration for the Mott transition has been estimated to be $(1.0–1.2)\times 10^{18}\ \mathrm{cm}^{-3}$ and $(3.3–7.1)\times 10^{18}\ \mathrm{cm}^{-3}$ in zb-GaN:Si and zb-AlN:Si, respectively.[15] The distribution of the impurity ions has been shown to be of major importance for the results,[9,16] and the present calculations are assuming a random distribution of impurities. Interactions with the nonionized impurity atoms are neglected. Since we are treating only the ionized impurities, the calculation does not depend on the choice of type of dopant atom.

The Coulomb potential $v(\mathbf{q}) = 4\pi e^2/\mathbf{q}^2$ of the electrons and the ionized impurities is screened by virtual transitions across the fundamental band gap, resulting in the screened Coulomb potential $v(\mathbf{q})/\kappa(\omega)$, where $\kappa(\omega)$ is the dielectric function of the intrinsic crystal (the lattice dielectric function). By including the Fröhlich's electron-optical-phonon coupling of large polarons and interpret the interaction as an additional screening of $v(\mathbf{q})$, the dielectric function is becoming frequency dependent also in the low-frequency regime.[12,17] The screened Coulomb potential comprises thereby not only the virtual transitions across the band gap, but also the electron-optical phonon scattering.

A. Self-energies

The self-energy $\hbar\Sigma_j(\mathbf{k},\omega)$ is expressed in terms of the unperturbed electron Green's function and of the testparticle–particle dielectric function $\tilde{\epsilon}(\mathbf{q},\omega)$ of the electron gas (given in Sec. II C). We use the Rayleigh–Schrödinger approximation,[12] yielding $\hbar\Sigma_j(\mathbf{k},\omega) \approx \hbar\Sigma_j(\mathbf{k},\zeta_j^0(\mathbf{k}))$, where $\zeta_j^0(\mathbf{k}) = E_j^0(\mathbf{k})/\hbar$.

The self-energies below are derived for *n*-type materials, but the corresponding expressions for *p*-type materials can be obtained easily by treating the holes as particles and the electrons as antiparticles. This means the self-energy $\hbar\Sigma_j(\mathbf{k},\zeta_j^0(\mathbf{k}))$ should be replaced by $-\hbar\Sigma_j(\mathbf{k},-\zeta_j^0(\mathbf{k}))$.

The unperturbed Green's function describes the propagation of a noninteracting electron in the crystal and $\tilde{\epsilon}(\mathbf{q},\omega)$ describes the response of the electron gas due to a perturbation of the electron distribution. The unperturbed, time-ordered Green's function is defined as

$$G_j^0(\mathbf{k},\omega) = \frac{\eta_j(\mathbf{k})}{\omega - \zeta_j^0(\mathbf{k}) - i\delta} + \frac{1-\eta_j(\mathbf{k})}{\omega - \zeta_j^0(\mathbf{k}) + i\delta}, \tag{1}$$

where δ is an infinitesimal, positive number and $\eta_j(\mathbf{k})$ is the occupation number. If the cell-periodic parts $u_{j\sigma}^0(\mathbf{k},\mathbf{r})$ of the Bloch functions are assumed to be slowly varying functions of $\mathbf{r}$, then scattering due to the electron–electron interaction $\hat{V}_{\mathrm{ee}}$ can be approximated by

$$\langle \mathbf{k},j;\mathbf{k}',j'|\hat{V}_{\mathrm{ee}}|\mathbf{k}',j';\mathbf{k},j\rangle \approx \frac{v(\mathbf{q})}{\kappa(\omega)}\Lambda_{j,j'}(\mathbf{k},\mathbf{k}') \tag{2}$$

$$\Lambda_{j,j'}(\mathbf{k},\mathbf{k}') = \frac{1}{2}\sum_{\sigma,\sigma'=\uparrow,\downarrow}\left|\int d\mathbf{r}\, u_{j\sigma}^0(\mathbf{k},\mathbf{r})\, u_{j'\sigma'}^0(\mathbf{k}',\mathbf{r})\right|^2, \tag{3}$$

where $\mathbf{q} = \mathbf{k}' - \mathbf{k}$ and $\Lambda_{j,j'}(\mathbf{k},\mathbf{k}')$ is the spin-independent overlap integral.

The Hartree–Fock exchange interaction of the electron gas is defined as the electron–electron interaction caused by the Pauli principle. Using the approximation of Eq. (2), the exchange part of the electron self-energy is given by[8,9,12,18]

Downloaded 12 Dec 2012 to 200.128.60.106. Redistribution subject to AIP license or copyright; see http://jap.aip.org/about/rights_and_permissions

$$\hbar\Sigma_j^x(\mathbf{k},\zeta_j^0(\mathbf{k}))=\int\frac{d\mathbf{q}}{(2\pi)^3}\int\frac{d\omega}{2\pi i}\frac{v(\mathbf{q})}{\kappa(\omega)}\sum_{j'}\Lambda_{j,j'}(\mathbf{k},\mathbf{k}')\times\Bigg\{G_{j'}^0(\mathbf{k}',\omega+\zeta_j^0(\mathbf{k}))+\frac{1}{2}\Bigg(\frac{1}{\omega+[\zeta_{j'}^0(\mathbf{k}')-\zeta_j^0(\mathbf{k})]-i\delta}-\frac{1}{\omega-[\zeta_{j'}^0(\mathbf{k}')-\zeta_j^0(\mathbf{k})]+i\delta}\Bigg)\Bigg\} \quad (4)$$

where the electrostatic self-interaction of the electron (the second term) has been subtracted.

In the Hartree–Fock equation, the direct Coulomb term of the electron repulsion is cancelled by treating the impurity ions as a uniform distribution of positive charges. The remaining Coulomb repulsion of the electrons is ascribed to the correlation interaction. The correlation self-energy can be written as[8,9,12,18]

$$\hbar\Sigma_j^c(\mathbf{k},\zeta_j^0(\mathbf{k}))=\int\frac{d\mathbf{q}}{(2\pi)^3}\int\frac{d\omega}{2\pi i}\frac{v(\mathbf{q})}{\kappa(\omega)}\left(\frac{1}{\tilde{\epsilon}(\mathbf{q},\omega)}-1\right)\times\sum_{j'}\Lambda_{j,j'}(\mathbf{k},\mathbf{k}')G_{j'}^0(\mathbf{k}',\omega+\zeta_j^0(\mathbf{k})). \quad (5)$$

Finally, the self-energy from the electron-ionized donor interaction, assuming a random distribution of the ions with infinitely large masses, is given by[8,9,17]

$$\hbar\Sigma_j^{\text{ion}}(\mathbf{k},\zeta_j^0(\mathbf{k}))=-\frac{N_D^+}{\hbar}\int\frac{d\mathbf{q}}{(2\pi)^3}\left(\frac{v(\mathbf{q})}{\kappa(0)\tilde{\epsilon}(\mathbf{q},0)}\right)^2\times\sum_{j'}\Lambda_{j,j'}(\mathbf{k},\mathbf{k}')G_{j'}^0(\mathbf{k}',\zeta_j^0(\mathbf{k})). \quad (6)$$

The electron–donor ion interaction describes the relaxation of the electrons around the ionized donors N_D^+ and the resulting inhomogeneity of the electron gas is thus comprised here. Since the cancellation of the direct Coulomb term already has been taken into account in the correlation energy, Eq. (6) describes the self-energy from the difference in the electron density between a system with uniform distribution of the ion charges and a system of point-like ions.

B. Electronic band structure of the intrinsic crystal

The energy dispersions $E_j^0(\mathbf{k})$ of the intrinsic crystals have been calculated using a full-potential linearized augmented plane wave (FPLAPW) method, within the generalized gradient approximation (GGA) to the density functional theory (DFT). A software program[19] with a fully relativistic Hamiltonian and with the correlation potential of Perdew and Wang[20] and the exchange potential of Engel and Vosko[21] was used. This exchange-correlation potential has been shown to give good energy dispersions for semiconductors with direct band gap, like InN and GaAs.[22,23] We have employed experimental values of the lattice constants and the internal lattice parameter: $a=3.190$ Å, $c=5.189$ Å, and $u=0.377$ for wz-GaN,[24] $a=3.110$ Å, $c=4.980$ Å, and $u=0.3821$ for wz-AlN,[24] $a=4.49$ Å for zb-GaN,[25] and $a=4.38$ Å for zb-AlN.[26]

TABLE I. Calculated and experimental (in brackets) band-gap energies E_g^0, position of the conduction-band minimum, crystal-field splitting Δ_{cf}, spin-orbit split-off energy Δ_{so}, and effective electron masses of the intrinsic crystals.

	GaN		AlN	
	wz	zb	wz	zb
Minimum	Γ	Γ	Γ	X
E_g^0 (eV)	2.50 3.55[a] (3.50,[b] 3.51[c])	2.41 3.44[a] (3.3,[d] 3.2[e])	5.04 6.05[a] (6.28[f])	4.23 5.17[a] (5.34[g])
Δ_{cf} (meV)	24.5 (29,[h] 39[i])		213	
Δ_{so} (meV)	4.7 (8,[h] 8[i])	10.4 (17[c])	12.5	18.4
$m_{c1,\perp}$ (m_0)	0.21 (0.22,[j] 0.222,[k] 0.23[l])	0.20	0.34	0.36
$m_{c1,\parallel}$ (m_0)	0.19	0.20	0.32	0.54

[a]Reference 27, LDA calculation with a quasiparticle band-gap correction.
[b]Reference 29.
[c]Reference 30.
[d]Reference 31.
[e]Reference 32.
[f]Reference 33.
[g]Reference 7.
[h]Reference 34.
[i]Reference 35.
[j]Reference 36.
[k]Reference 37.
[l]Reference 38.

Since the III nitrides lack inversion symmetry, the average spin-independent eigenvalues were obtained as $E_j^0(\mathbf{k})=[E_{j\uparrow}^0(\mathbf{k})+E_{j\downarrow}^0(\mathbf{k})]/2$ where ↑ and ↓ are the spin-up and spin-down-like states. More information of the electronic structure calculation of intrinsic GaN and AlN can be found in Refs. 27 and 28.

The DFT/GGA is well known to underestimate the fundamental band gap (see Table I).[7,27,29–38] However, one normally believes that the band curvatures can be described accurately by the GGA, at least for wide-band-gap semiconductors. The band curvatures of the lowest conduction band of all four crystals were found to be essentially parabolic in all direction in **k** space and in the energy regime of interest here. We, therefore, use ellipsoidal energy dispersions for these materials, described by the three principal effective electron masses (Table I). Our calculated effective masses are in good agreement with calculations performed by Stampfl and Van de Walle;[39] Städele *et al.*;[40] Vogel, Krüger, and Pollmann;[41] Park and Chuang;[42] Suzuki, Venoyama, and Yanase;[43] Ramos *et al.*;[44] Kim, Lambrecht, and Segall;[45] and Vurgaftman, Meyer, and Ram-Mohan.[30] In Table I we also show the corresponding measured values (in brackets).

The overlap integrals related to scattering within one and the same minimum of the lowest conduction band

Downloaded 12 Dec 2012 to 200.128.60.106. Redistribution subject to AIP license or copyright; see http://jap.aip.org/about/rights_and_permissions

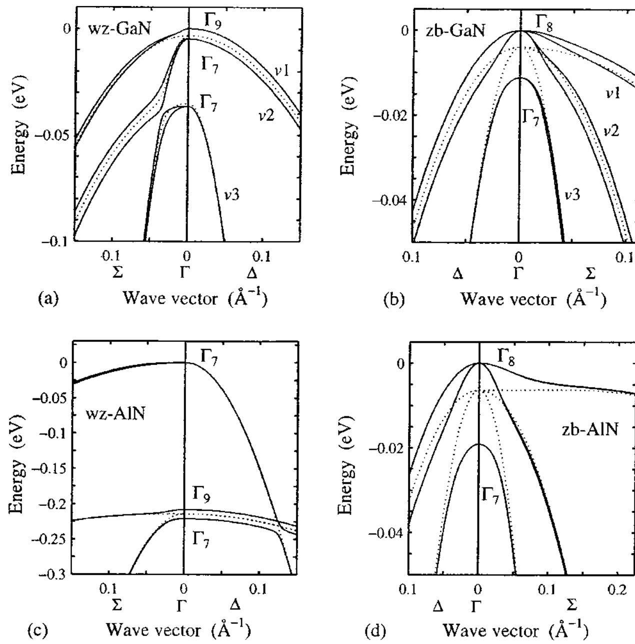

FIG. 1. Energy dispersions of the valence-band maximum in wz and zb GaN and AlN, obtained from a relativistic, full-potential LAPW calculation. The dotted lines represent the results in the absence of the spin-orbit coupling.

$\Lambda_{c1,c1}(\mathbf{k},\mathbf{k}')$ were found to be close to 1 for a set of **k** and **k**′ near the Γ point. Furthermore, it has been shown[16] that intervalley scattering between stats in different equivalent minima gives only a minor contribution to the self-energies for crystals with random distribution of impurities compared to the intravalley scattering. Intervalley scattering is, therefore, neglected in zb-AlN, which has three equivalent conduction-band minima located at the *X* points.

The energy dispersion of the valence-band maximum is in general very nonparabolic mainly because of the spin-orbit interaction. Also, the *p*-like valence bands have different curvatures in different **k**-space directions. In Fig. 1, the electronic structure near the valence-band maximum is shown along two symmetry directions. Moreover, due to the symmetry of the *p*-like eigenfunctions at the valence-band maximum, the energy bands of zb structures cannot be described by ellipsoidal functions even at the vicinity of the Γ point. In fact, the values of the effective hole masses at the Γ point depend very strongly on the **k** direction. In wz-GaN the nonparabolicity in the Σ direction is obvious for energies about 4 meV below the valence-band maximum. The uppermost valence band in wz-AlN (which is the crystal-field split-off band, in contrast to wz-GaN) is almost unaffected by the spin-orbit interaction, and therefore an ellipsoidal description of this band is sufficient. Noticeably, the valence-band maximum in zb-AlN is not at the Γ point if the spin-orbit interaction is excluded, whereas the fully relativistic calculation yields a maximum at the Γ point.

The energy dispersions of the three uppermost valence bands [i.e., $E_j^0(\mathbf{k})$, $j=v1$, $v2$, and $v3$] have been calculated and the energy bands are represented on a mesh of about 23 000 **k** points in the first Brillouin zone, mainly concentrated about the Γ point. For calculating the doping-induced energy shift of the valence-band maximum the relevant overlap integrals are $\Lambda_{v1,j}(\mathbf{0},\mathbf{q})$ with $j=v1$, $v2$, and $v3$. The overlap integrals are represented on the same mesh of **k** points as the energy bands.

C. Dielectric functions

The frequency-dependent lattice dielectric function $\kappa(\omega)$ is expressed in terms of the static $\kappa(0)$ and high-frequency $\kappa(\infty)$ limits. The phonons involved in the screening are the longitudinal optical (LO) phonons with long wavelengths,[12,17] approximated to have constant phonon dispersion $\hbar\omega_{\mathrm{LO}}$. The lattice dielectric function for isotropic materials is then given by[12,17]

$$\frac{1}{\kappa(\omega)}=\frac{1}{\kappa(\infty)}-\frac{[\kappa(0)-\kappa(\infty)]\omega_{\mathrm{LO}}}{2\kappa(0)\kappa(\infty)}\left(\frac{1}{\omega+\omega_{\mathrm{LO}}-i\delta}-\frac{1}{\omega-\omega_{\mathrm{LO}}+i\delta}\right). \tag{7}$$

We have employed experimental values[1] for the lattice dielectric function: $\hbar\omega_{\mathrm{LO}}=92$ meV, $\kappa(0)=9.98$, and $\kappa(\infty)=5.60$ for wz-GaN and $\hbar\omega_{\mathrm{LO}}=110$ meV, $\kappa(0)=9.14$, and $\kappa(\infty)=4.84$ for wz-AlN. Calculations of the phonon frequencies by Kim, Lambrecht, and Segall[46] are in close agreement with the measured values.[1,47–51]

The anisotropy of the dielectric function of the wz structures has been shown to be small in the materials considered here [$\kappa_\perp(0)=9.44$, $\kappa_\parallel(0)=9.62$, $\kappa_\perp(\infty)=5.76$, and $\kappa_\parallel(\infty)=5.88$ in GaN, and $\kappa_\perp(0)=7.91$, $\kappa_\parallel(0)=8.22$, $\kappa_\perp(\infty)=4.53$, and $\kappa_\parallel(\infty)=4.72$ in AlN],[27,47] and we therefore use the isotropic lattice dielectric functions. Moreover, we assume that the zb structures have the same lattice dielectric function as the corresponding wz structures. This assumption is supported by calculations of the optical properties of wz and zb III nitrides in Refs. 42, 46, and 52–54, and by spectroscopic ellipsometry measurements of Logothetidis *et al.*[50]

Within the RPA,[11,12] and with the local-field correction $\bar{f}(\mathbf{q})$, the testparticle–particle dielectric function of the electron gas (the hole gas, in the case of *p*-type doping) is related to the polarizability $\alpha^0(\mathbf{q},\omega)$ by[8,9,11]

$$\tilde{\epsilon}(\mathbf{q},\omega)=1+[1-\bar{f}(\mathbf{q})]\alpha^0(\mathbf{q},\omega), \tag{8}$$

$$\alpha^0(\mathbf{q},\omega)=-\frac{2}{\hbar}\frac{v(\mathbf{q})}{\kappa(\omega)}\int\frac{d\mathbf{k}}{(2\pi)^3}\int\frac{d\omega'}{2\pi i}\sum_{j,j'}\Lambda_{j,j'}(\mathbf{k},\mathbf{k}')\times G_j^0(\mathbf{k},\omega')G_{j'}^0(\mathbf{k}',\omega'+\omega), \tag{9}$$

where the summation runs over all conduction (valence) bands, which are populated by the electron (hole) gas. The free-electron (hole) concentration $n=N_D^+$ ($p=N_A^-$) fills the conduction band (valence bands) up (down) to the Fermi energy E_F^c (E_F^v). For *p*-type doping, the number of populated valence bands λ_v depends on the hole concentration.

In order to evaluate the integral for the polarizability and thereby get an analytic expression for $\alpha^0(\mathbf{q},\omega)$,[8,18] the energy dispersions of the Green's functions in Eq. (9) are approximated using ellipsoidal energy dispersions and setting the overlap integrals to unity. In this approximation the en-

Downloaded 12 Dec 2012 to 200.128.60.106. Redistribution subject to AIP license or copyright; see http://jap.aip.org/about/rights_and_permissions

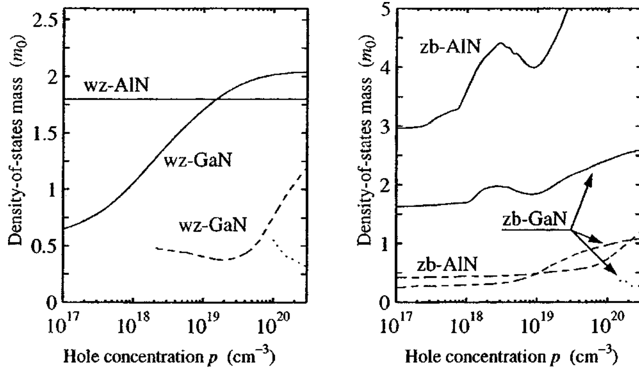

FIG. 2. Concentration-dependent density-of-states effective hole masses $m_{v1}(p)$ (solid lines), $m_{v2}(p)$ (dashed lines), and $m_{v3}(p)$ (dotted lines) used for calculating the polarizability $\alpha^0(\mathbf{q},\omega)$.

ergy bands are represented by the density-of-states effective masses.[8] This is a very reasonable approximation for n-type doping. However, for p-type doping one needs to include some effects from the nonparabolic behavior of the valence-band maximum. We have, therefore, used concentration-dependent density-of-states effective masses $m_{v1}(p)$, $m_{v2}(p)$, and $m_{v3}(p)$. These masses are chosen in such a way that the resulting Fermi energy of the hole gas E_F^v coincides with the Fermi energy obtained using the numerical energy dispersion from the full band-structure calculation. This way of treating the valence bands has been found to give accurate results.[8,55] The reason for that is directly related to the occupation number and of the poles of the Green's functions. An accurate description of the Fermi energy is more important for calculating the polarizability than having the exact description of the curvature of the energy bands. However, an accurate description of the energy bands is important for calculating the self-energies via Eqs. (4)–(6). The calculated carrier concentration density-of-states effective masses are presented in Fig. 2.

In wz-GaN the energy difference between the uppermost and the second uppermost valence band is $E^0_{v1}(\mathbf{0})-E^0_{v2}(\mathbf{0})=4.7$ meV (see Fig. 1), and for p-type doping the second uppermost valence band starts to be populated at about $p=3\times10^{18}$ cm^{-3}. The third uppermost valence band $[E^0_{v1}(\mathbf{0})-E^0_{v3}(\mathbf{0})=26.9$ meV$]$ starts to be populated at about $p=1\times10^{20}$ cm^{-3}. Since the corresponding energy differences in wz-AlN are large $[E^0_{v1}(\mathbf{0})-E^0_{v2}(\mathbf{0})=207$ meV and $E^0_{v1}(\mathbf{0})-E^0_{v3}(\mathbf{0})=219$ meV$]$, neither the second nor the third band will be populated for any concentration considered here. In zb-GaN and zb-AlN, the energy difference between the doubly degenerate uppermost valence bands at the Γ point and the third uppermost valence band is calculated to be $E^0_{v1,v2}(\mathbf{0})-E^0_{v3}(\mathbf{0})=10$ and 18 meV, respectively. The onset of populating the third uppermost valence band in zb-GaN is at about 1×10^{20} cm^{-3}. However, the uppermost valence band in zb-AlN is very flat (see Fig. 1), yielding a large onset for populating the third band (about 4×10^{20} cm^{-3}). These differences in the energy dispersions between the four crystals are reflected in the self-energies (see Sec. III).

The local-field correction is calculated according to Hubbard,[13] which mainly takes account of the exchange hole around the electron. For n-type materials the averaged local-field correction is[8]

$$\bar{f}(\mathbf{q})=\frac{1}{2\lambda_c^2}\sum_i \frac{E^0_{c1}(\Delta\mathbf{k}_i+\mathbf{q})}{E^0_{c1}(\Delta\mathbf{k}_i+\mathbf{q})+E_F^c},\quad i=1,2,...,\lambda_c, \quad (10)$$

where $\Delta\mathbf{k}_i=\mathbf{k}_i+\mathbf{k}_m$ is the vector between the λ_c different equivalent minima and one chosen conduction-band minimum at $\mathbf{k}_m$. Analogously, for p-type materials the averaged local-field correction is[8]

$$\bar{f}(\mathbf{q})=\frac{1}{2\lambda_v^2}\sum_j \frac{E^0_j(\mathbf{q})\cdot\theta(E^0_j(\mathbf{0})-E_F^v)}{E^0_j(\mathbf{q})+E_F^v},\quad j=v1,\ v2,\ v3, \quad (11)$$

where $\theta(x)$ is the unit step function.

III. RESULTS

A. *n*-type GaN and AlN

The doping-induced energy shifts of the conduction-band minimum ΔE_{c1} and of the valence-band maximum ΔE_{v1} in n-type materials are obtained as

$$\Delta E_{c1}=\mathrm{Re}[\hbar\Sigma^x_{c1}(\mathbf{k}_m,\zeta^0_{c1}(\mathbf{k}_m))+\hbar\Sigma^c_{c1}(\mathbf{k}_m,\zeta^0_{c1}(\mathbf{k}_m)) +\hbar\Sigma^{\mathrm{ion}}_{c1}[(\mathbf{k}_m,\zeta^0_{c1}(\mathbf{k}_m))], \quad (12)$$

$$\Delta E_{v1}=\mathrm{Re}[\hbar\Sigma^c_{v1}(\mathbf{0},\zeta^0_{v1}(\mathbf{0}))+\hbar\Sigma^{\mathrm{ion}}_{v1}(\mathbf{0},\zeta^0_{v1}(\mathbf{0}))]. \quad (13)$$

The shift of the valence band does not contain an exchange contribution since the band is fully occupied by electrons (apart from a few empty states needed for measuring the band gap and normally induced through excitation), and the exchange interaction is, therefore, already contained in the intrinsic valence-band structure. In Fig. 3, the energy shifts ΔE_{c1} and ΔE_{v1} as functions of the ionized donor concentration N_D^+ are presented (solid lines). The numerical error is below 1 meV. Comparison between the present RPA calculation and similar methods (the Hartree–Fock method, Thomas–Fermi method, etc.) has been discussed by, for instance, Mahan,[12] Berggren and Sernelius,[9] and Abram, Rees, and Wilson.[56]

The dashed lines in Fig. 3 represent the corresponding calculation with the approximation of using spherical energy dispersions of the valence bands, described by the constant density-of-states hole masses $m_j(p=0)$ with $j=v1$, $v2$, and $v3$. Furthermore, in this spherical approximation the overlap integrals of the valence bands are given by $\Lambda_{v1,j'}(\mathbf{0},\mathbf{q})=\delta_{v1,j'}$ for wz structures and $\Lambda_{v1,v1}(\mathbf{0},\mathbf{q})=[1+3\cos^2(\theta)]/4$, $\Lambda_{v1,v2}(\mathbf{0},\mathbf{q})=3\sin^2(\theta)/4$, and $\Lambda_{v1,v3}(\mathbf{0},\mathbf{q})=0$ for zb structures where θ is the angle between $\mathbf{q}$ and the k_x axis. The overlap integrals for the cubic crystals were derived by assuming spherical energy dispersions of the valence bands.[57]

The resulting reduced band-gap energy is obtained as $E_g=E_g^0+\Delta E_g=E_g^0+\Delta E_{c1}-\Delta E_{v1}$. The optical band gap is defined as the energy of zero-phonon-induced recombinations. For semiconductors with a direct band gap the optical band gap is given by $E_g^{\mathrm{opt}}=E_g+\Delta E_{\mathrm{BM}}$, where ΔE_{BM} is the Burstein–Moss shift,[58,59] which arises from the band filling, that is, the vertical transitions from the conduction-band

Downloaded 12 Dec 2012 to 200.128.60.106. Redistribution subject to AIP license or copyright; see http://jap.aip.org/about/rights_and_permissions

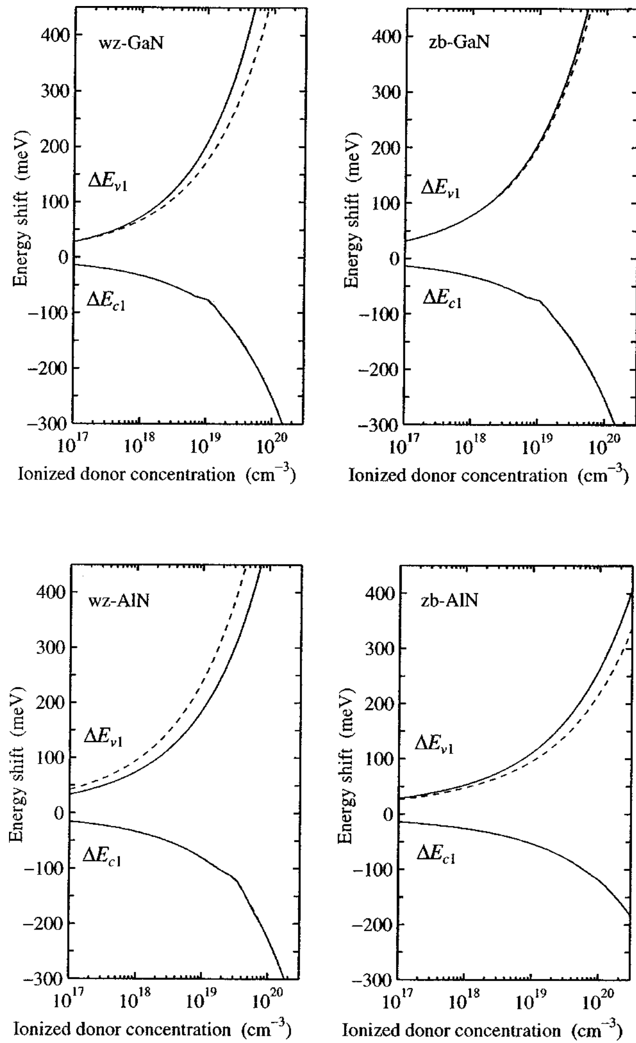

FIG. 3. Energy shift of the lowest conduction-band minimum ΔE_{c1} and of the uppermost valence-band maximum ΔE_{v1} in *n*-type wz-GaN, wz-AlN, zb-GaN, and zb-AlN. The solid lines represent the full band calculations, whereas dashed lines are corresponding calculations within the spherical approximation.

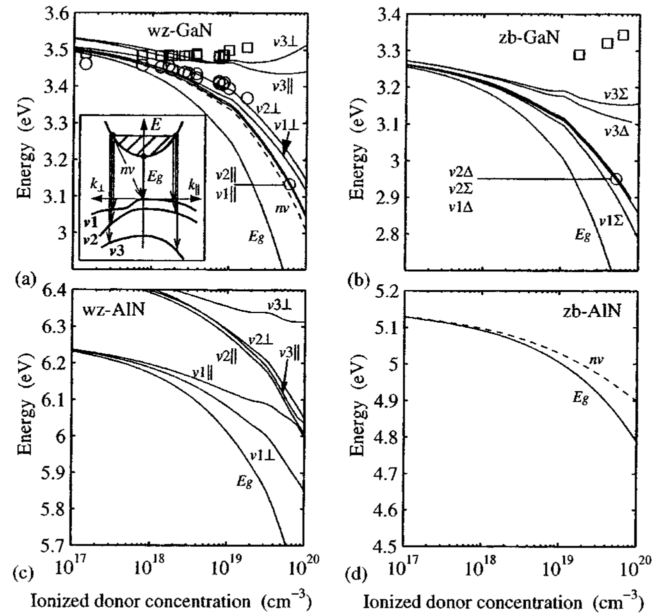

FIG. 4. Reduced band gap E_g, the **k**-dependent optical band gap (to the three valence bands $v1$, $v2$, and $v3$; cf. Fig. 1), and the nonvertical energy gap (*nv*, dashed line) in (a) wz-GaN, (b) zb-GaN, (c) wz-AlN, and (d) zb-AlN, obtained from the full band-structure calculation. The inset in (a) shows schematically the different transitions. The circles and squares in (a) represent the PL measurements of wz-GaN:Si by Yoshikawa *et al.* (Ref. 14), and the squares in (b) represent the PL measurements of wz-GaN:Si done by Fernandez *et al.* (Ref. 15).

states at E_F^c with the Fermi wave vector $\mathbf{k}_F$ to the corresponding **k** states of nonthermalized holes in the valence bands. Thus, for direct band-gap materials the Burstein–Moss shift is given by

$$\Delta E_{BM,j}(\mathbf{k}_F)=[(E_{c1}(\mathbf{k}_F)-E_{c1}(\mathbf{0}))]+[E_{v1}(\mathbf{0})-E_j(\mathbf{k}_F)] \quad \text{(direct band gap)}, \tag{14}$$

where $j=v1$, $v2$, $v3$, and $E_{c1}(\mathbf{k}_F)=E_F^c$. One needs the full **k** dependence of the energy dispersion of the valence bands in order to calculate the Burstein–Moss shift properly. For semiconductors with indirect band gap, there are no zero-phonon-induced recombinations since there are free electrons only at the conduction-band minimum. (The probability for vertical transitions is very small.) One, therefore, refers to the "optical band gap" as the nonvertical transitions from the Fermi energy to the thermalized hole state at the valence-band maximum. The Burstein–Moss shift is thus given by[58,59]

$$\Delta E_{\mathrm{BM}}=E_F^c-E_{c1}(\mathbf{0}) \quad \text{(indirect band gap)}. \tag{15}$$

In Fig. 4, we present the reduced band gap and the energy differences which correspond to transitions to the three uppermost valence bands ($v1$, $v2$, and $v3$) in two symmetry directions ($\perp$ and $\parallel$ for wz structures and Δ and Σ for zb structures). The inset in Fig. 4(a) shows schematically the different transitions. We assume no band distortion due to the doping.

The energy of the optical transitions in wz-GaN [Fig. 4(a)] depends strongly on the **k** vector of the recombining electron–hole pair. This is a result of the valence bands having a different energy dispersion along the transverse and the longitudinal directions, which is reflected in the Burstein–Moss shift, and thereby also in the optical band gap. Figure 4(a) shows only transitions in the two main symmetry directions, and, thus, a recombination in an arbitrary direction can have a recombination energy between the energy for the transverse and the longitudinal directions. In Fig. 4(a), we also present the nonvertical (*nv*) transition to the valence-band maximum (dashed line). The circles and squares are the low-energy and the high-energy cutoff PL results of Yoshikawa *et al.*,[14] obtained from a 1–2.5 μm Si-doped GaN layer on an undoped buffer GaN layer, using metal–organic chemical vapor deposition. In Ref. 14, an estimate of $\Delta E_g < 7$ meV due to strain is reported. It has been shown[60] that using constant hole masses for describing the energy dispersion, the PL results cannot be fully explained. However, with the full band structure, we can identify the PL results of Yoshikawa *et al.* as different vertical transitions to the three uppermost valence bands in different directions of the **k** space.

Downloaded 12 Dec 2012 to 200.128.60.106. Redistribution subject to AIP license or copyright; see http://jap.aip.org/about/rights_and_permissions

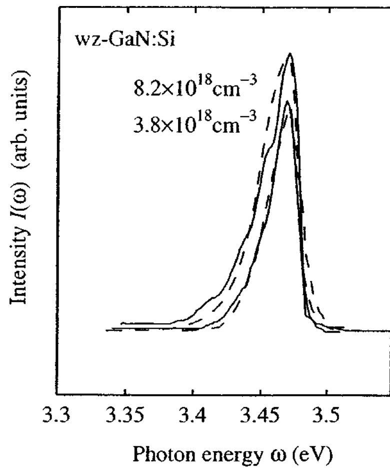

FIG. 5. Estimate (dashed lines) of the zero-phonon-induced transition probability [Eq. (17)] of wz-GaN:Si using the full band structure. The solid lines are the PL result of Yoshikawa *et al.* (Ref. 14) at the absolute temperature $T=2$ K.

Yoshikawa *et al.*[14] interpreted their results as originating from the reduced band-gap and nonvertical transitions to the valence-band maximum, thus without conservation of momentum. First, our calculated reduced band gap is much smaller than the energy of the low-energy PL edge. For $N_D^+ = 1\times10^{19}$ cm^{-3}, the calculated shift is about twice as large as the corresponding measured low-energy edge. Second, the phonon-induced nonvertical transitions are normally much less probable than the corresponding vertical transitions in semiconductors with direct band gap. According to Fig. 4(a), both the low-energy edge and the high-energy cutoff of the PL spectra can be explained as the zero-phonon-induced recombinations.

In order to strengthen the arguments that the PL results could come from vertical transitions, we have simulated the PL spectra of Yoshikawa *et al.*[14] by calculating the joint density-of-states weighted by the Fermi–Dirac distribution function $f_{\mathrm{FD}}(x)$ for the electrons and a chosen distribution function for the holes $f_v(E_j(\mathbf{k}))=\exp[-|E_j(\mathbf{k})+E_F^c - E_g|/\alpha]$:

$$I(\omega)=\sum_j \frac{1}{(2\pi)^3}\int \delta(\omega-[E_{c1}(\mathbf{k})-E_j(\mathbf{k})]) \times f_v(E_j(\mathbf{k}))f_{\mathrm{FD}}(E_{c1}(\mathbf{k}))d\mathbf{k}, \quad j=v1,v2,v3 \tag{16}$$

Thus, f_v favors a distribution of holes with wave vectors near $\mathbf{k}_F$ in order to simulate a transition probability which favors direct transitions. By fitting the parameter α to 0.008 eV we can reproduce the PL spectra fairly accurately for both $N_D^+=3.8\times10^{18}$ and 8.2×10^{18} cm^{-3} (see Fig. 5). Thus, our calculations suggest that the PL spectra of Yoshikawa *et al.* describe zero-phonon-induced recombinations between electrons at the Fermi level and nonthermalized holes in the different valence bands. We hope this result will motivate further investigations of band-gap shifts in wz-GaN:Si.

The calculated optical band gap of zb-GaN [Fig. 4(b)] is not in agreement with the PL measurements of Fernandez *et al.*[15] of zb-GaN:Si [squares in Fig. 4(b)]. Their results of $E_g^{\mathrm{opt}}=3.290$, 3.3208, and 3.343 eV for $N_D^+=1.7\times10^{19}$, 3.9×10^{19}, and 6.2×10^{19} cm^{-3}, respectively, are close to the band gap of intrinsic zb-GaN [$E_g^0=3.2$–3.3 eV (Refs. 31 and 32)]. Also, for zb-GaN, we hope our calculations will motivate further investigations.

The differences in the optical band-gap energies between wz-GaN and wz-AlN arise from the different valence-band maxima of the two crystals. In contrast to wz-GaN, the uppermost band in wz-AlN is the crystal-field split-off band, with a band maximum more than 200 meV above the second and the third uppermost bands. One can, therefore, expect that only the uppermost band is important for low electric field transport properties in wz-AlN. However, the shift of the reduced band gap is quite comparable in the two wz crystals.

The differences in both the reduced and the optical band gap between zb-GaN and zb-AlN arise mainly from the conduction band. wz-GaN has only one minimum, whereas zb-AlN has three equivalent minima that affect the band filling. Furthermore, the effective electron masses are larger in zb-AlN than in zb-GaN (see Table I). This makes the band-gap shift and the Burstein–Moss shift much smaller in zb-AlN.

B. *p*-type GaN and AlN

The doping-induced energy shifts of the conduction-band minimum ΔE_{c1} and of the valence-band maximum ΔE_{v1} in *p*-type materials are, according to the discussion in the previous sections, given by

$$\Delta E_{c1} = -\mathrm{Re}[\hbar\Sigma_{c1}^{c}(\mathbf{k}_m,-\zeta_{c1}^0(\mathbf{k}_m)) + \hbar\Sigma_{c1}^{\mathrm{ion}}(\mathbf{k}_m,-\zeta_{c1}^0(\mathbf{k}_m))], \tag{17}$$

$$\Delta E_{v1} = -\mathrm{Re}[\hbar\Sigma_{v1}^{x}(\mathbf{0},-\zeta_{v1}^0(\mathbf{0}))+\hbar\Sigma_{v1}^{c}(\mathbf{0},-\zeta_{v1}^0(\mathbf{0})) + \hbar\Sigma_{v1}^{\mathrm{ion}}(\mathbf{0},-\zeta_{v1}^0(\mathbf{0}))]. \tag{18}$$

In Fig. 6, the energy shifts ΔE_{c1} and ΔE_{v1} as functions of ionized acceptor concentration N_A^- are presented (solid lines). The dashed lines in Fig. 6 represent the spherical approximation of the energy dispersion and the overlap integrals. For low ionized acceptor concentrations the spherical approximation gives a fairly good description of the energy shifts. This is what could be expected, since the employed crystal parameters within the spherical approximation were chosen in order to describe the energy dispersion at the very top of the valence bands. For large hole concentrations, however, the spherical approximation of the valence bands fails to describe the true Fermi energy, and the resulting energy shifts differ from the results obtained using the numerical energy dispersions. The details in the curvatures of ΔE_{c1} and ΔE_{v1}, especially for the hexagonal crystals, can be explained directly from the energy dispersion of the three valence bands (cf. Sect. II C and Figs. 1 and 2). For different hole concentrations, the number of populated valence bands differs. This will have a direct consequence on the polarizability of the hole gas, and thus also affects the self-energies. Increasing the number of populated bands tends to reduce the band-gap shift.

Downloaded 12 Dec 2012 to 200.128.60.106. Redistribution subject to AIP license or copyright; see http://jap.aip.org/about/rights_and_permissions

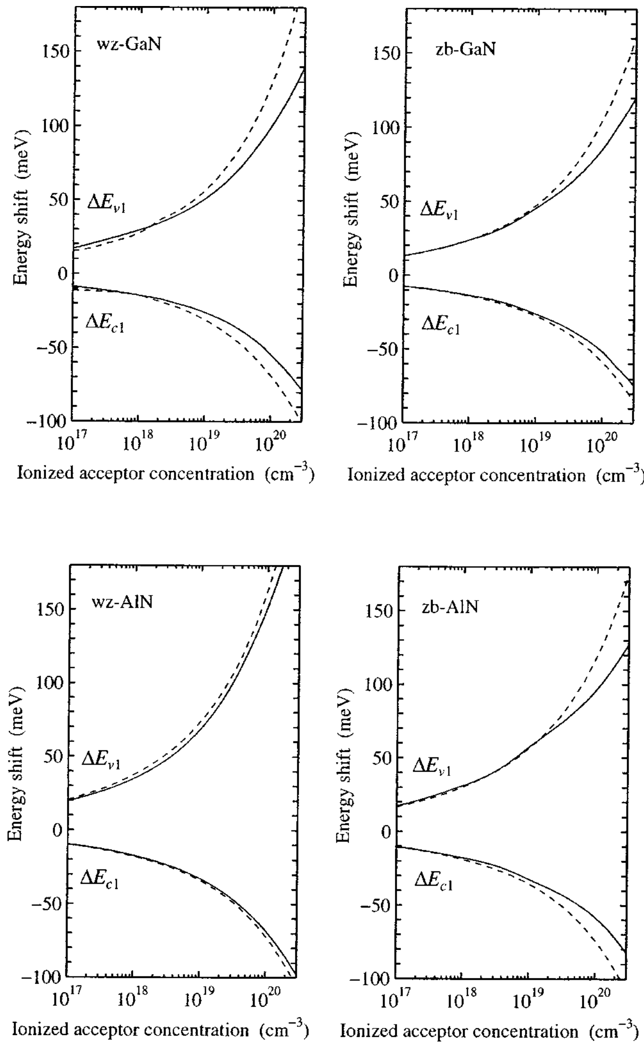

FIG. 6. Same as Fig. 3, but for *p*-type doping.

The resulting reduced band gap $E_g = E_g^0 + \Delta E_{c1} - \Delta E_{v1}$ and optical band gap E_g^{opt} in *p*-type doped GaN and AlN are shown in Fig. 7. The optical band gap is obtained as the zero-phonon-induced recombinations, except in the case of zb-AlN where the indirect recombinations are assumed to occur between the states at $\mathbf{k}_F$ in the valence bands to the conduction-band minimum at the *X* point (cf. Sec. III A). The inset in Fig. 7(d) shows schematically the different transitions. There are no experimental results for the doping-induced band-gap narrowing in *p*-type GaN or AlN.

The effects on the optical band gap due to the nonparabolicity can be seen in Figs. 7(b) and 4(b) for zb-GaN. The spherical approximation would result in the same transition energies in the Σ direction as in the Δ direction ($v1\Sigma = v1\Delta$ and $v2\Sigma = v2\Delta$) since the effective mass tensor is considered to be constant (i.e., spherical mass). The full band-structure calculations yield, however, completely different results. Moreover, in the calculations of Ref. 60, spherical energy dispersion is used also for the hexagonal structures. That resulted in $v1\perp = v1\|$ and $v2\perp = v2\|$, which can be compared to the corresponding results in Figs. 7(a), 7(c), 4(a), and 4(c).

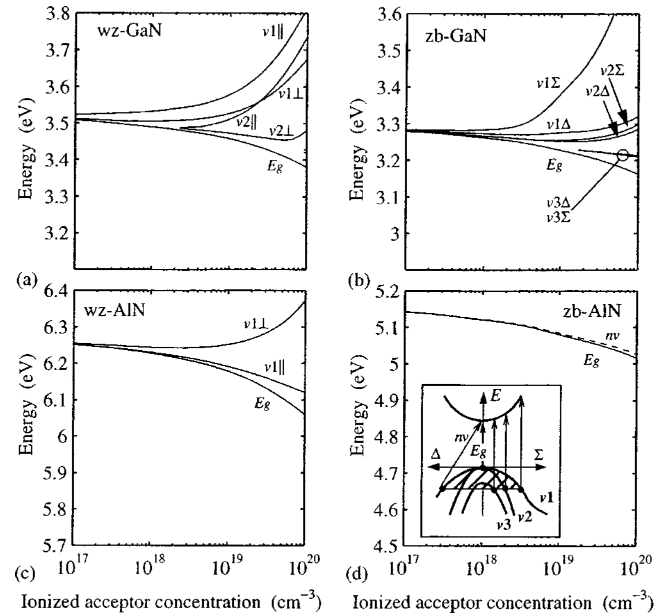

FIG. 7. Same as Fig. 4, but for *p*-type doping.

By comparing Figs. 7 and Fig. 4, one notices that the shift of the reduced band gap is much smaller in *p*-type doped GaN and AlN (for both zb and wz structures) than in corresponding *n*-type doped materials. Moreover, from Fig. 6, it is clear that the nonparabolicity reduces the energy shift. We have seen this effect also in *p*-type Si and in *p*-type GaAs.[23,55] Like in the case of *n*-type doping, the differences in the optical band gap between GaN and AlN (for both zb and wz structures) arise mainly from the different valence-band maxima of the crystals. Since we now also have band filling of the valence bands (which yields a screening caused by the hole gas), the differences are more pronounced for *p*-type doping than for corresponding *n*-type doping.

In wz-AlN, neither the second nor the third uppermost valence band contribute to the hole-gas polarizability. Since there are no empty states in these valence bands, we do not expect optical transitions from these bands. In wz-GaN, optical recombinations between states in the conduction band states in the uppermost valence band (in both the [100] and the [001] directions) as well as in the second uppermost valence band (in the [001] direction) result in large photon energies. Thus, the nonparabolicity has a strong effect on the reduced band gap in *p*-type materials, and on the optical band gap in both *n*- and *p*-type materials, except in the case of wz-AlN which has a parabolic valence-band maximum.

The very flat curvature (i.e., the large density of states) of the uppermost valence band in zb-AlN results in a very low Fermi energy, and thus the optical band gap (here, the nonvertical transitions) is close to the reduced band gap. In zb-GaN, it is the uppermost valence band in the [110] direction that yields the largest shift of the optical band gap.

IV. SUMMARY AND DISCUSSION

The doping-induced energy shifts of the lowest conduction-band minimum and the uppermost valence-band

Downloaded 12 Dec 2012 to 200.128.60.106. Redistribution subject to AIP license or copyright; see http://jap.aip.org/about/rights_and_permissions

maximum have been calculated for *n*- and *p*-type wz-GaN, wz-AlN, zb-GaN, and zb-AlN using the RPA with the Hubbard local-field correction. The spin-orbit interaction affects the energy dispersion of the uppermost valence bands, and we have shown that the nonparabolicity of the bands has a strong impact on the resulting self-energies. Similar results have been reported for *p*-type Si and GaAs,[23,55] where better agreement between calculations and measurements was obtained with a full description of the valence bands.

With the full band-structure calculation of the reduced and the optical band-gap energies, we have identified the PL spectra of Yoshikawa *et al.*[14] as zero-phonon-induced recombinations of electrons in the conduction band and nonthermalized holes in the three uppermost valence bands.

In the calculations of the optical band gap, we assumed that the band curvatures, for describing the band filling, are not modified by the doping. However, it has been shown[28] that for very high-impurity concentration there will be a band tailing in GaN and AlN, mainly due to the polaron coupling. This band distortion will increase the optical band-gap energy slightly. From Ref. 28, we can estimate this effect in *n*-type GaN to be less than 8 and 25 meV for $N_D^+ = 1\times10^{18}$ and 1×10^{19} cm^{-3}, respectively.

Strain has an important role in the growth of the nitrides. Strain is also technologically interesting since it can suppress Auger recombinations. In the present work, we have investigated the band-gap narrowing of unstrained materials only. In the PL measurements on wz-GaN of Yoshikawa *et al.*,[14] the affect on the band gap due to strain is estimated to be smaller than 7 meV.

The method of calculating the band-gap shifts was based on a zero-temperature formalism and the results are in a strict sense valid only for impurity concentration above the concentration for the MNM transition, which is about $(1.0-1.2)\times10^{18}$ cm^{-3} in zb-GaN:Si and $(3.3-7.1)\times10^{18}$ cm^{-3} in zb-AlN:Si.[15] For *n*-type Si, a finite-temperature RPA calculation has been performed by Sernelius[61] and by Thuselt and Rösler,[62] showing that the zero-temperature calculation is a good approximation for calculations of ΔE_{c1} even at finite temperatures, mainly due to compensating effects between the correlation and the exchange interactions. However, in *n*-type (*p*-type) materials ΔE_{v1} (ΔE_{c1}) does not depend on the exchange energy and this shift might, therefore, be more affected by the temperature. Nevertheless, it is believed that the zero-temperature calculations presented here can, with reasonable accuracy, be applied for finite temperatures for concentrations below the Mott transition where the impurities are partly or fully ionized thermally.

ACKNOWLEDGMENTS

This work was financially supported by the Swedish Research Council (VR), ATOMICS funded by the Swedish Foundation for Strategic Research (SSF), the U.S. Department of Energy under Contract No. DE-AC05-00OR22725 with Oak Ridge National Laboratory, managed by UT-Battelle, LLC, and the Brazilian National Research Council (CNPq).

[1] S. Strite and H. Morkoc, J. Vac. Sci. Technol. B **10**, 1237 (1992).
[2] S. C. Jain, M. Willander, J. Narayan, and R. Van Overstraeten, J. Appl. Phys. **87**, 965 (2000).
[3] S. Nakamura, M. Senoh, N. Iwasa, S. Nagahama, T. Yamada, and T. Mukai, Jpn. J. Appl. Phys., Part 2 **34**, L1332 (1995).
[4] M. Asif Khan, J. N. Kuznia, A. R. Bhattarai, and D. T. Olson, Appl. Phys. Lett. **62**, 1786 (1993).
[5] O. Brandt, in *Group III Nitride Semiconductor Compounds*, edited by B. Gil (Clarendon, Oxford, 1998).
[6] D. Schikora, M. Hankeln, D. J. As, K. Lischka, T. Litz, A. Waag, T. Buhrow, and F. Henneberger, Phys. Rev. B **54**, 8381 (1996).
[7] M. P. Thompson, G. W. Auner, T. S. Zheleva, K. A. Jones, S. J. Simko, and J. N. Hilfiker, J. Appl. Phys. **89**, 3331 (2000).
[8] C. Persson, U. Lindefelt, and B. E. Sernelius, Phys. Rev. B **60**, 16479 (1999).
[9] K.-F. Berggren and B. E. Sernelius, Phys. Rev. B **24**, 1971 (1981).
[10] N. F. Mott, *Metal–Insulator Transitions* (Taylor and Francis, London, 1974).
[11] A. A. Kugler, J. Stat. Phys. **12**, 35 (1975).
[12] G. D. Mahan, *Many-Particle Physics*, 2nd ed. (Plenum, New York, 1990).
[13] J. Hubbard, Proc. R. Soc. London, Ser. A **243**, 336 (1957).
[14] M. Yoshikawa, M. Kunzer, J. Wagner, H. Obloh, P. Schlotter, R. Schmidt, N. Herres, and U. Kaufmann, J. Appl. Phys. **86**, 4400 (1999).
[15] J. R. L. Fernandez, C. Moysés Araújo, A. Ferreira da Silva, J. R. Leite, Bo E. Sernelius, A. Tabata, E. Abramof, V. A. Chitta, C. Persson, R. Ahuja, I. Pepe, D. J. As, T. Frey, D. Schikora, and K. Lischka, J. Cryst. Growth **231**, 420 (2001).
[16] K.-F. Berggren and B. Sernelius, Phys. Rev. B **29**, 5575 (1984).
[17] B. E. Sernelius and K.-F. Berggren, Philos. Mag. B **43**, 115 (1981).
[18] T. M. Rice, Ann. Phys. **31**, 100 (1965).
[19] P. Blaha, K. Schwarz, and J. Luitz, in WIEN97, A Full Potential Linearized Augmented Plane Wave Package for Calculating Crystal Properties, Karlheinz Schwarz, Technical Universität, Wien, Austria, 1999.
[20] J. P. Perdew and Y. Wang, Phys. Rev. B **45**, 13244 (1992).
[21] E. Engel and S. H. Vosko, Phys. Rev. B **50**, 10498 (1994).
[22] C. Persson, R. Ahuja, A. Ferreira da Silva, and B. Johansson, J. Phys.: Condens. Matter **13**, 8945 (2001).
[23] C. Persson, R. Ahuja, and B. Johansson, Phys. Rev. B **64**, 033201 (2001).
[24] H. P. Maruska and J. J. Tietjen, Appl. Phys. Lett. **15**, 327 (1969).
[25] T. Lei, M. Fanciulli, R. J. Molnar, T. D. Moustakas, R. J. Graham, and J. Scanlon, Appl. Phys. Lett. **59**, 944 (1991).
[26] I. Petrov, E. Mojab, R. C. Powell, J. E. Greene, L. Hultman, and J.-E. Sundgren, Appl. Phys. Lett. **60**, 2491 (1992).
[27] C. Persson, A. Ferreira da Silva, R. Ahuja, and B. Johansson, J. Cryst. Growth **231**, 397 (2001).
[28] C. Persson, B. E. Sernelius, A. Ferreira da Silva, R. Ahuja, and B. Johansson, J. Phys.: Condens. Matter **13**, 8915 (2001).
[29] B. Monemar, Phys. Rev. B **10**, 676 (1974).
[30] I. Vurgaftman, J. R. Meyer, and L. R. Ram-Mohan, J. Appl. Phys. **89**, 5815 (2001).
[31] G. Ramirez-Flores, H. Navarro-Contreras, A. Lastras-Martinez, R. C. Powell, and J. E. Greene, Phys. Rev. B **50**, 8433 (1994).
[32] T. Lei, T. D. Moustakas, R. J. Graham, Y. He, and S. J. Berkowitz, J. Appl. Phys. **71**, 4933 (1992).
[33] P. B. Perry and R. F. Rutz, Appl. Phys. Lett. **33**, 319 (1978).
[34] W. A. Harrison, *Electronic Structure and the Properties of Solids* (Freeman, San Francisco, 1980).
[35] D. Volm, K. Oettinger, T. Streibl, D. Kovalev, M. Ben-Chorin, J. Diener, B. K. Meyer, J. Majewski, L. Eckey, A. Hoffmann, H. Amano, I. Akasaki, K. Hiramatsu, and T. Detchprohm, Phys. Rev. B **53**, 16543 (1996).
[36] M. Drechsler, D. M. Hofmann, B. K. Meyer, T. Detchprohm, H. Amano, and I. Akasaki, Jpn. J. Appl. Phys., Part 2 **34**, L1178 (1995).
[37] A. M. Witowski, K. Pakula, J. M. Baranowski, M. L. Sadowski, and P. Wyder, Appl. Phys. Lett. **75**, 4154 (1999).
[38] Y. J. Wang, R. Kaplan, H. K. Ng, K. Doverspike, D. K. Gaskill, T. Ikedo, I. Akasaki, and H. Amono, J. Appl. Phys. **79**, 8007 (1996).
[39] C. Stampfl and C. G. Van de Walle, Phys. Rev. B **59**, 5521 (1999).
[40] M. Städele, M. Moukara, J. A. Majewski, P. Vogl, and A. Görling, Phys. Rev. B **59**, 10031 (1999).
[41] D. Vogel, P. Krüger, and J. Pollmann, Phys. Rev. B **55**, 12836 (1997).
[42] S.-H. Park and S.-L. Chuang, J. Appl. Phys. **87**, 353 (2000).
[43] M. Suzuki, T. Uenoyama, and A. Yanase, Phys. Rev. B **52**, 8132 (1995).
[44] L. E. Ramos, L. K. Teles, L. M. R. Scolfaro, J. L. P. Castineira, A. L.

Downloaded 12 Dec 2012 to 200.128.60.106. Redistribution subject to AIP license or copyright; see http://jap.aip.org/about/rights_and_permissions

Rosa, and J. R. Leite, Phys. Rev. B **63**, 165210 (2001).
[45] K. Kim, W. R. L. Lambrecht, and B. Segall, Phys. Rev. B **56**, 7363 (1997).
[46] K. Kim, W. R. L. Lambrecht, and B. Segall, Phys. Rev. B **53**, 16 310 (1996).
[47] R. Goldhahn, S. Shokhovets, J. Scheiner, G. Gobsch, T. S. Cheng, C. T. Foxon, U. Kaiser, G. D. Kipshidze, and W. Richter, Phys. Status Solidi A **177**, 107 (2000).
[48] G. Brockt and H. Lakner, Micron **31**, 435 (2000).
[49] L. X. Benedict, T. Wethkamp, K. Wilmers, C. Cobet, N. Esser, E. L. Shirley, W. Richter, and M. Cardona, Solid State Commun. **112**, 129 (1999).
[50] S. Logothetidis, J. Petalas, M. Cardona, and T. D. Moustakas, Phys. Rev. B **50**, 18017 (1994).
[51] T. Kawashima, H. Yoshikawa, S. Adachi, S. Fuke, and K. Ohtsuka, J. Appl. Phys. **82**, 3528 (1997).
[52] C. Persson, R. Ahuja, A. Ferreira da Silva, and B. Johansson, J. Cryst. Growth **231**, 407 (2001).
[53] K. Karch, J.-M. Wagner, and F. Bechstedt, Phys. Rev. B **57**, 7043 (1998).
[54] J.-M. Wagner and F. Bechstedt, Phys. Rev. B **62**, 4526 (2000).
[55] C. Persson, U. Lindefelt, and B. Sernelius, J. Appl. Phys. **86**, 4419 (1999).
[56] R. A. Abram, G. J. Rees, and B. L. H. Wilson, Adv. Phys. **27**, 799 (1978).
[57] M. Combescot and P. Nozières, Solid State Commun. **10**, 301 (1972).
[58] E. Burstein, Phys. Rev. **93**, 632 (1954).
[59] T. M. Moss, Proc. Phys. Soc. London, Sect. B **67**, 775 (1954).
[60] A. Ferreira da Silva, C. Moysés Araújo, Bo E. Sernelius, C. Persson, R. Ahuja, and B. Johansson, J. Phys.: Condens. Matter **13**, 8891 (2001).
[61] B. E. Sernelius, *Proceedings of the 3rd International Conference on Shallow Impurities in Semiconductors*, Linköping, Ser. No. 95, p. 137 (IOP, Bristol, 1988).
[62] F. Thuselt and M. Rösler, Phys. Status Solidi B **130**, 661 (1985).

Downloaded 12 Dec 2012 to 200.128.60.106. Redistribution subject to AIP license or copyright; see http://jap.aip.org/about/rights_and_permissions